High-throughput screening for half-metallic double perovskites

Supervisor: Prof Jinlong Yang, USTC. Manuscript in preparation.

Half-metallic ferromagnets,[1] as 100% polarized spin sources, are superior to previous spin injectors with fractional spin polarization. Candidates for half-metallicity include Eu chalcogenides,[2–4] transition metal pnictides and chalcogenides in zincblend structure[5–7], magnetites,[8] CrO_2[9] and other oxides such as cuprate $Sr_8CaRe_3Cu_4O_{24}$,[10] $NaSr_5Cr_3Os_3O_{18}$[11] and ZrCuSiAs-type $La(Mn_{0.5}Zn_{0.5})AsO$,[12] two-dimensional materials such as transition-metal-doped CNTs[13] and MnO_2 nanosheets with Mn vacancies,[14] DMS-like materials such as Cr-doped β-SiC[15] and Cr-doped Cd_3As_2[16] and manganites,[17] Heusler compounds,[1,18] and double perovskites.[19,20]

Several issues need to be addressed for half-metallic ferromagnets to be practical spintronic materials. In order to fabricate room-temperature spintronic devices, transition temperatures at which materials lose half-metallicity should be higher than RT, a requirement that has been met in Heusler compounds and double perovskites.[21] Secondly, magnetic anisotropy facilitates the alignment of spins in the presence of thermal fluctuations, which is important for stability in data storage. Thirdly, in order to prevent possible spin-flip transitions that could destroy half-metallicity below the Curie temperature, wide half-metallic peaks with Fermi energy close to minority-spin valence band maximum is desirable.[22,23]

In order to address these issues, we utilized high-throughput computational screening to identify half-metals with large minority-spin band gaps, strong magnetic anisotropy and high Curie temperatures. High-throughput DFT+U calculation was carried out on 1600 double perovskites $AA'BB'O_6$ (A,A'=La,Ba,Sr; B,B'=transition metal). Electronic structures, magnetic coupling and magnetic anisotropy energy were calculated. Candidates were screened according to the figures of merit. Due to the fact that PBE+U tends to favor a half-metallic phase, hybrid functional HSE06 calculations are carried out to validate the results for selected half-metallic candidates. A number of half-metallic double perovskites with significantly improved figures of merit have been identified, and we also present an analysis on the difficulties of and potential solutions to optimizing figures of merit.

Theoretical calculations were performed based on first-principles density functional theory (DFT) method with the PBE generalized gradient approximation (GGA) implemented in Vienna ab initio Simulation Package (VASP). During the high-throughput screening process, the strong-correlated correction is considered with GGA+U method. The effective onsite Coulomb interaction parameters U and J are taken from a number of papers on the same subject. The projector augmented wave (PAW) potential and the plane-wave cutoff energy of 400 eV are used. The convergence criterion for the total energy is set as 1×10^{-5} eV. In order to validate the results of the high-throughput screening, electronic structures and figures of merit of the selected candidates were recalculated. PBE+U is used for the geometry optimization. Criteria for energy and forces are set as 1×10^{-5} eV and 0.01 ev/Å respectively, and energy cutoff is 450 eV. Hybrid functional HSE06 is used for energy, electronic structure and magnetic anisotropy calculation. Electronic structures are calculated with an energy convergence criterion of 1×10^{-6} eV. Magnetic anisotropy energies are calculated with an energy cutoff of 500 eV and energy convergence criterion of 1×10^{-7} eV. A 2×1×1 supercell is used to calculate magnetic coupling constants.

Three figures of merit are used in the screening process. The minority spin bandgap is defined as the energy range in which density of states is 0 for the minority spin (minority spin here refers to the spin orientation with zero density of states at the Fermi level), illustrated in Figure 1. The magnetic anisotropy energy is characterized by the standard deviation of the energies when spins align along the direction <001>, <100> and <100>. The Curie temperature is (at the time of writing) characterized by the energy difference between ferromagnetic and antiferromagnetic configurations. The Curie temperature T_C can be calculated using the two dimensional Ising Model, using $k_B T_C = c \times J$, where J the exchange constant.

In the screening process, full structural optimization and density of states calculation are carried out for each candidate. Half-metallic candidates are selected from 1600 double perovskites, and minority spin band gaps are extracted. The exchange constants are then computed for each candidate, and candidates with ferromagnetic ground states are selected. Magnetic anisotropy energy is then calculated.

A typical optimized structure of a double perovskite $A_2BB'O_6$ is shown in Figure 1, and consist of AO layers and $BB'O_2$ layers. Chemical bonding within octahedral coordination is primarily of a covalent nature. For B and B' ions, the splitting of bonding and antibonding orbitals competes against strength of magnetic coupling to determine magnetism and electronic structure. Also, magnetic couplings happen primarily within layers.

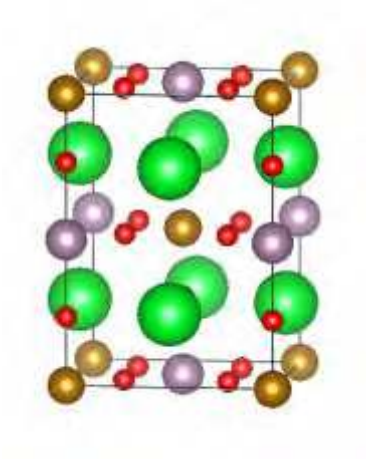

Figure 1 Typical crystal cell of a double perovskite

The figures of merit of double perovskite $AA'BB'O_6$ are plotted against atomic numbers of B and B' in Figure 2, Figure 3 and Figure 4. Figures of merit of the best candidates are compared against those in a previous JACS paper[12] in Figure 5. The usual value for magnetic anisotropy energy and minority-spin bandgap is of the order of 0.1 meV and 1eV respectively, and such figures of merit as reported here are rather rare. The significantly improved figures of merit show promises for practical half-metallic double perovskite materials as spintronic materials.

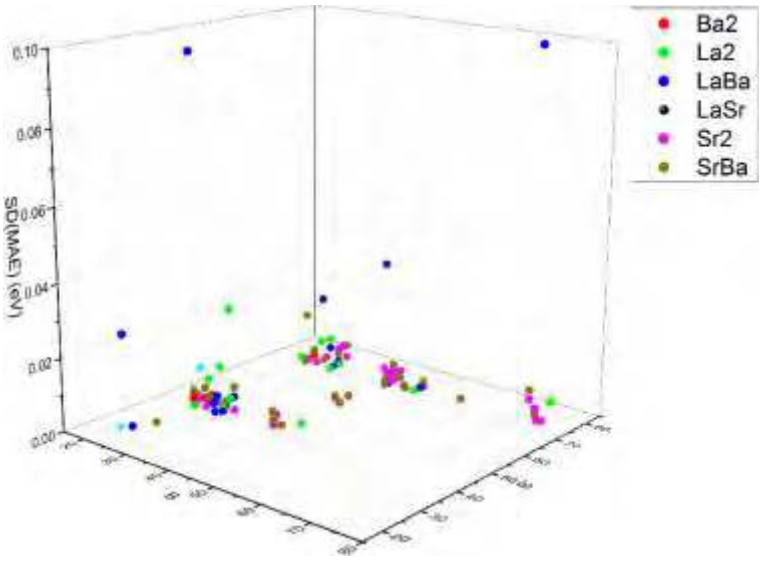

Figure 2 Magnetic Anisotropy Energy plotted against atomic numbers

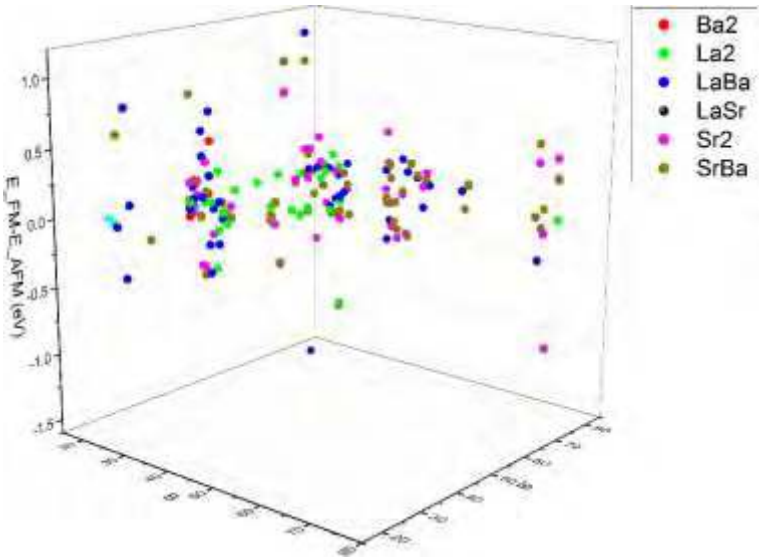

Figure 3 E_{FM}-E_{AFM} plotted against atomic numbers

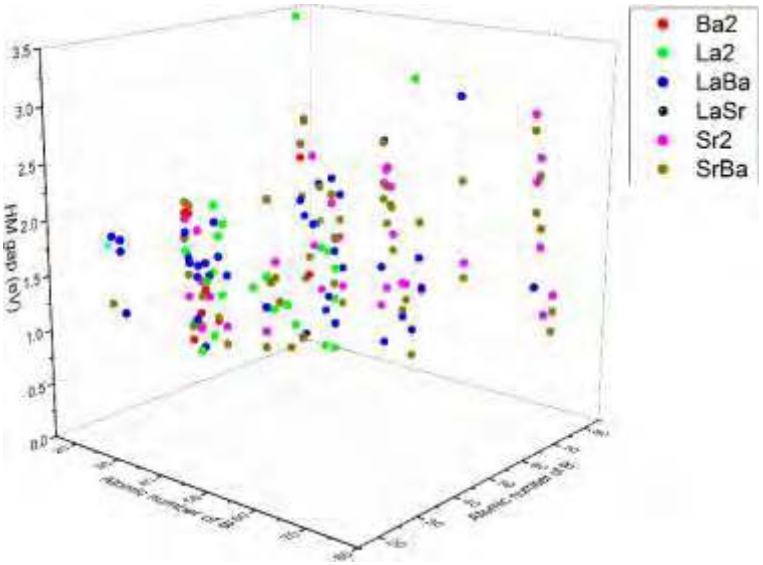

Figure 4 Minority spin gap plotted against atomic numbers

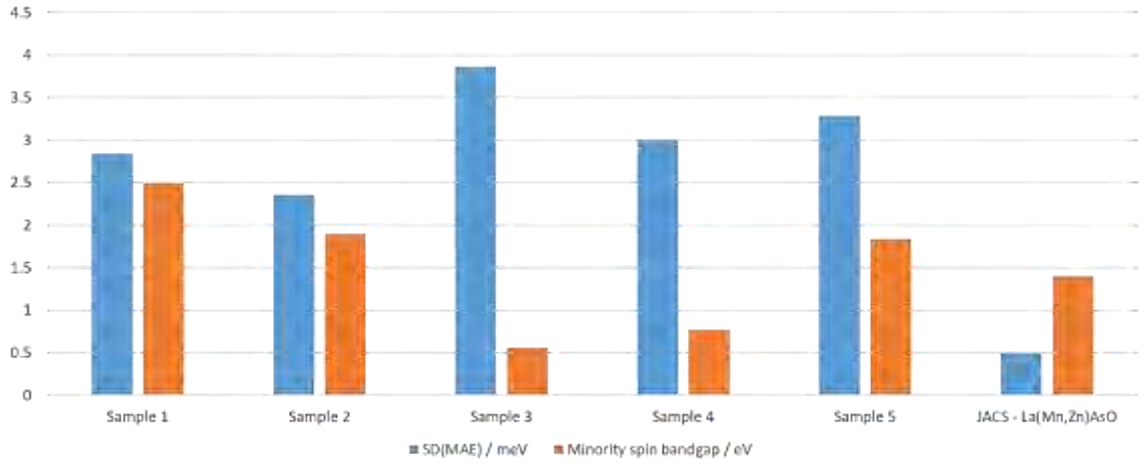

Figure 5 Figures of merit of double perovskite AA'BB'O6

Next, I attempt to present a simple discussion of difficulties against designing a half-metallic double perovskite with all figures of merit optimal. Firstly, the Heisenberg model dictates that atomic magnetism is most likely for 3d transition metal atoms due to restrictions on atomic radii. Unfortunately, magnetic anistropy energy tends to be small for the lighter 3d atoms. Secondly, half-metallicity is a sensitive electronic property depending upon the relative energies of orbitals to the Fermi level. As the minority-spin band gap is of the order of 1 eV, small numerical deviances and real-world perturbations easily destroys the ideal 100% spin polarization. In addition, the position of the majority spin orbital strongly depends upon the strength of magnetic coupling and correlation. Both could prove difficult to tune quantitatively. Nevertheless, regulating the electronic structures is theoretically possible. For instance, one could engineer the Fermi level by applying a gate voltage, or by electron or hole doping. The overlap of O 2p orbital and metal d orbitals has also been shown

to cause half-metallicity. Steric effects, by affecting bonding strength and the energy difference between bonding and antibonding orbitals, might prove instrumental. The rich physics in perovskite materials encourages one to explore the structure-property relationship in more depth to optimize the figures of merit.

In conclusion, using high-throughput computational screening approaches, we identified several half-metallic double perovskites with significantly improved figures of merit for spintronic applications, including magnetic anisotropy energy, minority-spin bandgap and Curie temperatures. While an interplay of factors present obstacles to achieving optimal values for all figures of merit, an overall improvement is theoretically possible either through brute-force approaches or by drawing on the structure-property relationships to regulate electronic structures. Other practical issues, such as the prevention of spin-flip transition and decomposition into parasite phases in synthesis, are also prospective topics of investigation in order to realize practical spintronic devices based on half-metallic ferromagnets.

(1) Groot, R. De; Mueller, F. M. M.; de Groot, R. A.; Mueller, F. M. M.; Engen, P. G. van; Buschow, K. H. J. Phys. Rev. Lett. **1983**, 50 (25), 2024–2027.

(2) Moodera, J. S.; Meservey, R.; Hao, X. Phys. Rev. Lett. **1993**, 70 (6), 853.

(3) Moodera, J. S.; Hao, X.; Gibson, G. A.; Meservey, R. Phys. Rev. Lett. **1988**, 61 (5), 637.

(4) Santos, T. S.; Moodera, J. S. Phys. Rev. B **2004**, 69 (24), 241203.

(5) Liu, B.-G. In Half-metallic Alloys; Springer, 2005; pp 267–291.

(6) Xie, W.-H.; Xu, Y.-Q.; Liu, B.-G.; Pettifor, D. G. Phys. Rev. Lett. **2003**, 91 (3), 37204.

(7) Galanakis, I.; Mavropoulos, P. Phys. Rev. B **2003**, 67 (10), 104417.

(8) Von Molnár, S.; Read, D. Proc. IEEE **2003**, 91 (5), 715–726.

(9) Coey, J. M. D.; Venkatesan, M. J. Appl. Phys. **2002**, 91 (10), 8345–8350.

(10) Wan, X.; Kohno, M.; Hu, X. Phys. Rev. Lett. **2005**, 95 (14), 146602.

(11) Zu, N.; Wang, J.; Wang, Y.; Wu, Z. J. Alloys Compd. **2015**, 636, 257–260.

(12) Li, X.; Wu, X.; Yang, J. J. Am. Chem. Soc. **2014**, 136, 5664–5669.

(13) Kan, E.; Li, Z.; Yang, J. Nano **2008**, 03 (06), 433.

(14) Yi, J. B.; Lim, C. C.; Xing, G. Z.; Fan, H. M.; Van, L. H.; Huang, S. L.; Yang, K. S.; Huang, X. L.; Qin, X. B.; Wang, B. Y.; Wu, T.; Wang, L.; Zhang, H. T.; Gao, X. Y.; Liu, T.; Wee, a. T. S.; Feng, Y. P.; Ding, J. Phys. Rev. Lett. **2010**, 104 (April), 1–4.

(15) Kim, Y.; Chung, Y. October **2005**, 41 (10), 2733–2735.

(16) Jin, H.; Dai, Y.; Ma, Y.-D.; Li, X.-R.; Wei, W.; Yu, L.; Huang, B.-B. J. Mater. Chem. C **2015**, 3 (15), 3547–3551.

(17) Bowen, M.; Maurice, J.-L.; Barthélémy, a; Bibes, M.; Imhoff, D.; Bellini, V.; Bertacco, R.; Wortmann, D.; Seneor, P.; Jacquet, E.; Vaurès, a; Humbert, J.; Contour, J.-P.; Colliex, C.; Blügel, S.; Dederichs, P. H. J. Phys. Condens. Matter **2007**, 19 (31), 315208.

(18) Alijani, V.; Winterlik, J.; Fecher, G. H.; Naghavi, S. S.; Felser, C. Phys. Rev. B **2011**, 83 (18), 184428.

(19) Kobayashi, K.-I.; Kimura, T.; Tomioka, Y.; Sawada, H.; Terakura, K.; Tokura, Y. Phys. Rev. B **1999**, 59 (17), 11159.

(20) Kobayashi, K.-I.; Kimura, T.; Sawada, H.; Terakura, K.; Tokura, Y.; Kobayashi, K.-I.; Kimura, T.; Sawada, H.; Terakura, K.; Tokura, Y. Nature **1998**, 395 (October), 677–680.

(21) Meetei, O. N.; Erten, O.; Mukherjee, A.; Randeria, M.; Trivedi, N.; Woodward, P. **2012**, 1–8.

(22) Hordequin, C.; Ristoiu, D.; Ranno, L.; Pierre, J. Eur. Phys. J. B **2000**, 16, 287–293.

(23) Fong, C. Y.; Qian, M. C.; Liu, K.; Yang, L. H. **2007**.